

Is MC Dropout Bayesian?

Loïc Le Folgoc¹, Vasileios Baltatzis², Sujal Desai^{1,3}, Anand Devaraj³, Sam Ellis³, Octavio E. Martinez Manzanera², Arjun Nair⁴, Huaqi Qiu¹, Julia Schnabel², and Ben Glocker¹

¹ BioMedIA, Imperial College London, United Kingdom

² Biomedical Engineering and Imaging Sciences, King’s College London, UK

³ The Royal Brompton & Harefield NHS Foundation Trust, London UK

⁴ Department of Radiology, University College London, UK

`l.le-folgoc@imperial.ac.uk`

Abstract. MC Dropout is a mainstream “free lunch” method in medical imaging for approximate Bayesian computations (ABC). Its appeal is to solve out-of-the-box the daunting task of ABC and uncertainty quantification in Neural Networks (NNs); to fall within the variational inference (VI) framework; and to propose a highly multimodal, faithful predictive posterior. We question the properties of MC Dropout for approximate inference, as in fact MC Dropout changes the Bayesian model; its predictive posterior assigns 0 probability to the true model on closed-form benchmarks; the multimodality of its predictive posterior is not a property of the true predictive posterior but a design artefact. To address the need for VI on arbitrary models, we share a generic VI engine within the pytorch framework. The code includes a carefully designed implementation of structured (diagonal plus low-rank) multivariate normal variational families, and mixtures thereof. It is intended as a go-to no-free-lunch approach, addressing shortcomings of mean-field VI with an adjustable trade-off between expressivity and computational complexity.

1 Introduction

The Bayesian framework provides a formalism for probabilistic predictions given partial knowledge of a potentially biased model of the real-world, and limited observations. Uncertainty quantification can improve risk assessment and decision making. It is especially relevant in medical imaging, given the complex relationship between the low-level processing (often performed sequentially) and the downstream, high-level patient management. Applications span segmentation [18,10], registration [19,8,13,20] and model personalisation [12,17,5]. Crucial to Bayesian UQ is Bayesian modelling: ultimately the probabilistic model has to be faithful to the phenomenon it describes. Even moderately complex models bring forth computational challenges, hence second to faithful modelling is faithful approximate Bayesian computation (ABC). ABC engines aim at approximating intractable posterior distributions. Our main message is a warning against the misuse of MC dropout for ABC. We show that the MC dropout approximate posterior poorly fits the original model and is essentially non-Bayesian.

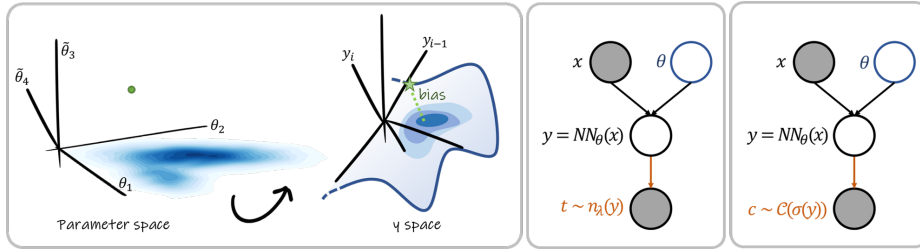


Fig. 1. (Left) The predictive error is due to a combination of model discrepancy/bias and within-model uncertainty. E.g. parameters $\tilde{\theta}_3, \tilde{\theta}_4$ fail to be accounted for by a 2-parameter model. The true model (green dot) is not reachable by the parametrization θ_1, θ_2 . Reachable solutions lie on a 2D manifold (green star \equiv true value). The predictive posterior on y (blue shades, y -space) reflects within-model uncertainty, *i.e.* uncertainty on the model parameters captured in the posterior (blue shades, θ -space). (Middle) Standard Bayesian model of regression, resp. (Right) classification. Within-model uncertainty has epistemic (\equiv blue node) and aleatoric (\equiv orange arrow) sources.

The predictive error (Fig. 1 left) is the combination of an out-of-model component, the model *discrepancy* or *bias* [11] w.r.t. the real-world; and a within-model uncertainty whose nature is partly *aleatoric* (due to noisy observations), partly *epistemic* (due to unknown model parameters). Consider the regression model of Fig. 1 (middle), whereby a variable of interest y results from some process $NN_\theta(x)$ that depends on inputs x and unknown parameters θ . Given this model choice and a dataset of noisy observations $\{X, T\}$, the knowledge of y_* for new inputs x_* is optimally described⁵ by the predictive posterior distribution:

$$p(y_*|x_*, X, T) = \int_{\theta} p(y_*|x_*, \theta) p(\theta|X, T) d\theta, \quad (1)$$

which weighs the likelihood $p(y_*|x_*, \theta)$ by the posterior probability $p(\theta|X, T)$ and sums over all possible values of $\theta \in \Omega$ in the parameter space. In general Eq. (1) has no closed-form and gives rise to a combinatorial problem. Several approximation strategies have been proposed, including Maximum A Posteriori inference, Markov Chain Monte Carlo [3,4,7], Expectation Propagation [16,23] and Variational Inference [26]. A common approach is to draw samples θ_k from the posterior $p(\theta|X, T)$ or from an approximation $q(\theta)$, followed by Monte Carlo integration, yielding:

$$p(y_*|x_*, X, T) \simeq \frac{1}{K} \sum_{1 \leq k \leq K} p(y_*|x_*, \theta_k). \quad (1')$$

When using an approximate posterior $q(\theta)$, the approximating family conditions the quality of the approximation. The family should be easy to sample from, rich enough to closely match the true posterior without making it overly challenging

⁵in the sense of Bayesian risk minimization

for optimizers to find a good fit q^* . VI approaches (incl. MC dropout [6]) can be analysed in light of the corresponding choice of q (sections 2,3). We compare MC dropout to alternative variational approximations: MAP, mean-field (MF-VI, with diagonal-covariance normal distributions), and finally structured normal distributions (sN-VI) or mixtures thereof (sGMM-VI). We contribute the variational engine for the latter (section 4).

2 Variational Inference And MC Dropout

VI aims to obtain a distribution $q(\theta) \in \mathcal{Q}$ that best fits the true posterior among the chosen variational family \mathcal{Q} , so as to exploit predictive estimates like Eq. (1'). VI proceeds by maximizing the Evidence Lower-BOund (ELBO):

$$\begin{aligned} \mathcal{L}(q) &\triangleq \log p(X, T) - \text{KL} [q(\theta) \| p(\theta|X, T)] , & (2) \\ &= \langle \log p(T|X, \theta) + \log p(\theta) \rangle_q + H(q) + \text{cst.} , & (2') \end{aligned}$$

where $H(q) = -\langle \log q \rangle_q$ is the entropy of q . Eq. (2) establishes the equivalence between maximizing the ELBO and minimizing the (positive) Kullback-Leibler divergence between true and variational posteriors. Eq. (2') makes the connection with standard penalized optimization clear. Observations $\{x_n, t_n\}$, $n = 1 \dots N$, are often assumed *i.i.d.*, so that the gradient of $\log p(T|X, \theta) = \sum_n \log p(t_n|x_n, \theta)$ splits into individual sample contributions. Thus SGD and variants, using unbiased mini-batch gradient estimates, are suitable optimizers for the ELBO. By specifying the variational family \mathcal{Q} we retrieve various approaches.

MAP. $q(\theta) \triangleq \delta_{\hat{\theta}}(\theta)$ for some $\hat{\theta} \in \Omega$. q places all the probability mass at $\hat{\theta}$. The expectation in Eq. (2') collapses into the point evaluation at $\hat{\theta}$. $H(q)$ is a constant ($-\infty$). The global optima for $\hat{\theta}$ are the global mode(s) of $p(\theta|X, T)$.

Mean Field. q is non-parametric but $q(\theta) \triangleq \prod_i q_i(\theta_i)$ factorizes over parameters θ_i , with generalizations to groupwise factorizations. The local extrema satisfy a set of coupled equations $\log q_i^*(\theta_i) = \langle f(X, T, \theta) \rangle_{q_{j \neq i}^*}$ that are closed form for hierarchical conjugate exponential models. This suggests iterative optimization of individual factors as in VBEM [1]. Alternatively q_i can be chosen among parametric families, leading to a computationally convenient subcase of what follows.

Parametric VI. $q(\theta) \triangleq q_\psi(\theta)$ is a parametric family indexed by ψ e.g., for multivariate normal distributions $\psi = (\mu, \Sigma)$ are the mean and covariance matrix. Optimization is done on ψ^* . The *Bayes by Backprop* strategy [2] combines stochastic gradient backpropagation with the *reparametrization* trick. The trick uses an equivalent functional form for random draws $\theta = f(z, \psi)$ from q_ψ , using draws z from a parameter-free distribution and an a.-e. differentiable f . E.g. $\theta = \mu + Lz$ with $\Sigma = LL^T$ and $z \sim \mathcal{N}(0, I)$ in the Gaussian case. An unbiased estimate of Eq. (2') is formed by Monte Carlo integration, replacing the expectation with an empirical average built from draws θ_k ; and backpropagated end-to-end

onto the variational parameters ψ . Applied to P -dimensional NN parameters, the strategy is subject to the curse of dimensionality as ψ can have a large memory footprint e.g., a full-rank covariance matrix has $\mathcal{O}(P^2)$ parameters; and the variance of the stochastic gradients can cause convergence issues, calling for more samples and model evaluations. This creates an effective trade-off between simplicity and richness of the variational family.

Implicit distributions. The approach uses the functional form $\theta := f(z; \psi) \triangleq f_\psi(z)$ with $z \sim p_z$ a random draw from a standard parameter-free distribution, to implicitly define the variational distribution $q(\theta)$. The flexibility in the mapping f_ψ (say, using NNs) allows to capture and sample from complex distributions more faithful to the true posterior. Unfortunately, $H(q)$ in Eq. (2') involves the log-density $\log q(f_\psi(z))$ of the *pushforward* distribution $q(\theta)$ of p_z by the map f_ψ , and is non-trivial to evaluate, giving rise to dedicated strategies [14,9,21,25]. These techniques have unparalleled expressivity but currently involve sophisticated training strategies or limiting constraints such as invertibility of f_ψ .

MC dropout. $q(\theta)$ is more easily described in an algorithmic way, as a sampling procedure for Monte Carlo integration of Eq. (2'). A binary variable $z_i \sim \mathcal{B}(p)$ and a weight $\hat{\theta}_i$ are attached to every NN parameter θ_i . At each iteration z_i 's are sampled, and $\theta_i := \hat{\theta}_i z_i$ is forced down to 0 if $z_i = 0$, set to $\hat{\theta}_i$ otherwise. $\hat{\theta}$ is optimized by stochastic backpropagation. The process mimics the training of dropout architectures [22]. Sampling proceeds similarly at test time to get an MC estimate Eq. (1'). Mathematically there are 2^P joint states for $z \triangleq (z_i)_i$, with probabilities $\triangleq q(z)$ modulated by the activation probability p , yielding a mixture of delta-Dirac variational posterior parametrized by $\hat{\theta}$:

$$q(\theta) = \sum_{1 \leq i \leq P} \sum_{z_i=0,1} \underbrace{\delta_{(\hat{\theta}_1 z_1, \dots, \hat{\theta}_P z_P)}(\theta_1, \dots, \theta_P)}_{\text{point mass at } \hat{\theta} \odot z} \cdot \underbrace{p^{\sum z_i} (1-p)^{\sum 1-z_i}}_{q(z) \text{ of joint state } z}, \quad (3)$$

where \odot stands for elementwise multiplication. The MC dropout predictive posterior, with $q(\theta)$ replacing $p(\theta|X, T)$ in Eq. (1), follows in closed form as:

$$p_{\text{MC-dropout}}(y_*|x_*, X, T) = \sum_{z \in [0,1]^P} p(y_*|x_*, \hat{\theta} \odot z) \cdot q(z) \quad (4)$$

3 Is MC Dropout Bayesian?

As shown in Fig. 2, MC dropout approximations fail sanity checks in a similar way to MAP approximations, in that they only assign non-zero probability to a finite set of parameters θ . In addition it is a modal approximation, hence sensitive to points of high posterior rather than to regions of high probability mass (Fig. 2, right). The resulting predictive posterior is illustrated in Fig. 3 in toy NN regression examples. All of the probability mass is distributed on a finite set of models (Eq. (4)), and the true model is assigned 0 probability. This contrasts with all other choices of variational families.

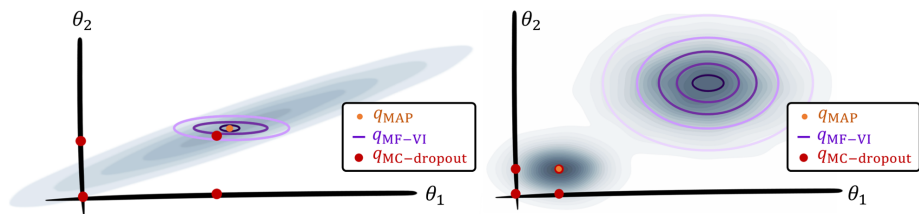


Fig. 2. 2D illustration of variational posterior fits, when the true posterior is unimodal (Left) or bimodal (Right). The true posterior is displayed as a blue-grey probability heatmap. Delta-Dirac masses are displayed as dots (MC dropout in red, MAP in orange). The MAP δ -Dirac is at the posterior mode. MC dropout is a mixture of $2^2 = 4$ δ -Dirac masses. The Gaussian MF-VI fit is displayed as axis-aligned isocontours.

Mean-field (MF-VI) approximations have non-degenerate probability density functions but cannot capture covariance between parameters, hence are known to suffer from uncertainty under-estimation. This is best seen from Fig. 2 where the Gaussian MF-VI posterior is restricted to axis-aligned isolines (ellipsoids). Full-covariance normal distributions have the expressivity to capture parameter covariance. Structured-covariance normal VI (sN-VI) lie within the two extremes, with $\Sigma = \text{diag}(A) + UU^T$ where $U \in \mathbb{R}^{P \times K}$ is low-rank ($K \ll P$). These models are unimodal approximations and fit complex multimodal posteriors poorly. Mixture models address this limitation.

MC dropout always yields a multimodal posterior (Eq. (3)(4)), even when the true posterior is unimodal. Despite being multimodal, it only has a single P -dimensional degree of freedom $\hat{\theta}$ that decides the mass distribution: delta-Dirac point-masses are located at $\hat{\theta}$ and at its (orthogonal) projections on every 1D axis, 2D plane, ..., $(P - 1)$ D hyperplane through the origin. This is a design artefact unrelated to the properties of the Bayesian model or of the data. In particular MC dropout does not have the expressivity to capture multimodal posteriors with its single degree of freedom $\hat{\theta}$ (Fig. 2, right). Moreover as the strategy would clearly be ill-suited for NN bias parameters, for which MC dropout therefore reverts to a standard δ -Dirac pointwise estimate.

Alternative interpretation. The MC dropout posterior is controlled by an arbitrary probability p of neuron activation. When $p := 1$, the posterior coincides with a MAP approximation q_{MAP} , whereas $p := 0$ places all the mass at the origin $\hat{\theta} = 0$. In practice the user manually chooses a value that optimizes say, accuracy. Rather than a technique for ABC, we can interpret the MC dropout strategy as modifying the original Bayesian model with a sparsity-inducing prior. Each parameter θ_i is attached a Bernoulli variable $z_i \sim \mathcal{B}(p)$. Then MC dropout follows as a naive approximation $q(\theta, z) = \delta_{\hat{\theta}}(\theta)p_z(z)$, whereby a (non-Bayesian) modal approximation is used on θ and z is sampled according to the prior p_z (instead of fitting say, $q(z) = \prod_i \mathcal{B}(z_i; p_i)$ or a logistic normal).

4 No Free Lunch Variational Inference

We contribute an engine for parametric VI based on the reparametrization trick and stochastic backpropagation⁶, with an implementation of structured multivariate normal families (sN-VI) and mixtures thereof (sGMM-VI). These are low-parametric families that capture parameter covariance within and across layers (and sGMM is multimodal). The implementation uses the pytorch framework, and reuses the design of the tool *pyvarinf* [24] to “variationalize” an arbitrary input model (e.g. NN). *Pyvarinf* implements Gaussian MF-VI. It rebuilds and evaluates the model on the fly (on a minibatch) with the sampled parameters θ after drawing from the variational posterior $q_{\psi,i}(\theta_i) = \mathcal{N}(\theta_i; \mu_i, \sigma_i)$, so that the model is seamlessly autodifferentiable w.r.t. ψ . We extend the mechanism to use arbitrary variational families q_ψ , given a functional rule $\theta = f(z, \psi)$ to draw one or multiple samples; and an evaluation of the log-density $\log q_\psi(\theta)$ or of the entropy $H(q_\psi)$. To initialize variational parameters, the default behaviour exploits heuristics based on the weight initialization routines of the original pytorch layers. As a training objective, one typically combines the MC estimate of the ELBO in Eq. (2') with any out-of-the-box stochastic gradient optimizer. The prior $p(\theta)$ is a Bayesian modelling choice and arbitrary. We provide examples using l_2 -regularization, (quasi) scale-invariant Student-t distributions and/or end-to-end Lipschitz regularization of the feature maps.

sN-VI and sGMM-VI have been proposed by Miller et al. [15] in the context of iterative, incremental refinement of an existing variational posterior. The authors leverage computational gains via low-rank (Woodbury) matrix identities, which we exploit as well. We depart from the literature based on the observation that standard stochastic backpropagation exhibits convergence issues even on sanity checks and with simple low-parametric families like sN. To stabilize gradient updates, the implementation proposes *paired* and *unscented* modes whereby coupled samples are drawn at once, in place of the naive reparametrization trick. In the paired mode, twin samples symmetrized around the mean are drawn. The unscented mode draws K coupled samples that use jointly orthogonal random combinations of the K low-rank directions, and their twin symmetric; somewhat reminiscent of unscented Kalman filtering. This disambiguates contributions of the mean, diagonal and low-rank covariance terms in the gradient updates. In addition we advocate as in [2] the use of $\log q_\psi(\theta_k)$ with the sampled θ_k 's in the Monte Carlo integration of Eq. (2') rather than say, the closed-form entropy $H(q_\psi)$ even when it is available. It reduces the variance of stochastic updates by letting draw-dependent scaling effects affect equally all terms.

5 Examples

Gaussian distribution fit. To validate the implementation of the variational engine, we fit a random multivariate 8-dimensional normal distribution $p =$

⁶The code is available at <https://github.com/llefolgo/dlvi>

$\mathcal{N}(\mu_0, \Sigma_0)$ via MAP, Gaussian MF-VI and various low-rank (from 1 to 8) structured normal distributions sN-VI $_{l_r}$. Table 1 reports the Kullback-Leibler divergence $\text{KL}[p||q]$ from the true distribution p to the variational posterior q . The pointwise MAP approximation yields an infinite divergence. MC-dropout is the only variational method not natively able to handle this sanity check (although a naive application of section 2 yields $\text{KL}[p||q] = +\infty$). As expected, the various sN-VI $_{l_r}$ are natural in-between approximations between a diagonal approximation like MF-VI (= sN-VI $_0$) and a full-covariance approximation like sN-VI $_8$.

	MAP	MC-drop.	MF-VI	sN-VI $_1$	sN-VI $_2$	sN-VI $_4$	sN-VI $_8$
$\text{KL}[p q]$	$+\infty$	—	175.8051	37.9890	25.9107	0.8774	0.0979

Table 1. Quality of fit $\text{KL}[p||q]$ of various variational approximations to a multivariate normal.

RBF regression. To illustrate the mechanism behind MC-dropout stochasticity we fit a small RBF 1-layer model in absence of model bias. Namely, let c_k , $1 \leq k \leq K = 10$, a set of regularly spaced basis centers. Let the true model $y = f(x) \triangleq \sum_{1 \leq k \leq 10} K(c_k, x)\theta_k^*$ a radial basis function with the $\theta_k^* \sim \mathcal{N}(0, 1)$ sampled randomly from a Gaussian distribution. Observations $t_n = y_n + \epsilon_n$, $\epsilon_n \sim \mathcal{N}(0, \sigma^2)$, $\sigma := 0.25$, are drawn with Gaussian noise, forming a training dataset $\{X, T\} = \{x_n, t_n\}_{n \leq N}$. Since the MC-dropout algorithm has no native mechanism to jointly fit the aleatoric noise, we assume the noise model known for simplicity. The full model is a one-layer linear model, $\mathbf{y} = \Pi_{\mathbf{c}}(\mathbf{x})\theta$, with $\mathbf{y} = (y_n)_{n \leq N}$, $\theta = (\theta_k)_{k \leq K}$, and $\Pi_{\mathbf{c}}(\mathbf{x})$ the matrix of (n, k) -th coefficient $K(c_k, x_n)$. We again fit the model with various methods, from MAP and MC-dropout to MF-VI and sN-VI. At training time, MC dropout fits a set $\hat{\theta}$ of weights by randomly dropping some components to 0 in $\theta := \hat{\theta} \odot \mathbf{z}$ with z_k 's randomly set to 0 or 1.

Fig. 3 summarizes the MC-dropout posterior as a set of $2^{10} = 1024$ delta-Dirac functions, a.k.a. "samples", generated by the $\theta^{(s)} := \hat{\theta} \odot \mathbf{z}^{(s)}$, $1 \leq s \leq 1024$, obtained from the various combinations of 0 and 1's as per section 2. None of the delta Dirac functions coincide with the true model (*i.e.* $\theta^{(s)} \neq \theta^*$ for all s). Thus the true model has 0 probability under the MC-dropout approximation. Under Gaussian variational approximations $q(\theta) = \mathcal{N}(\theta|\mu_v, \Sigma_v)$ instead, considering $N_* > K$ (unseen) test points $\{X_*, Y_*\}$, the probability of the true model $\mathbf{y}_* = \Pi_{\mathbf{c}}(\mathbf{x}_*)\theta^*$ is $\mathcal{N}(\theta^*|\mu_v, \Sigma_v) = q(\theta^*) \neq 0$.

Finally the exact posterior for θ is closed form as $p^* \triangleq p(\theta|X, T) = \mathcal{N}(\mu, \Sigma)$, $\Sigma \triangleq (\sigma^{-2}\Pi_{\mathbf{c}}(X)^T\Pi_{\mathbf{c}}(X) + \mathbf{I})^{-1}$, $\mu = \sigma^{-2}\Sigma\Pi_{\mathbf{c}}(X)^T\mathbf{t}$. The quality of approximation $\text{KL}[p^*||q]$ of the approximate posteriors $q(\theta)$ is also reported in Table 2. All Gaussian variational approximations perform similarly here.

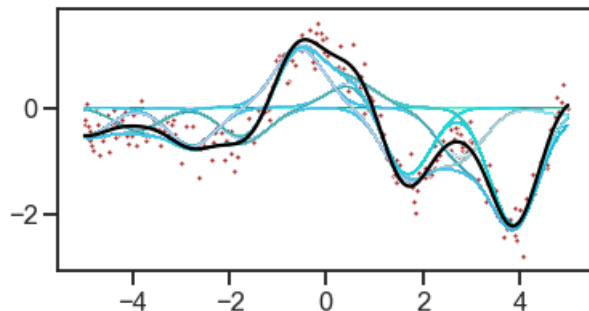


Fig. 3. MC-dropout posterior on 1-layer RBF regression. Black line: true model. Brown dots: observations. Blue lines are not samples from the approximate posterior, but the set of 1024 delta-Dirac functions forming the multimodal MC-dropout posterior. Evidently the location of the modes is unrelated to the model uncertainty and is instead simply an artefact of the MC-dropout approximation.

	MAP	MC-drop.	MF-VI	sN-VI ₁	sN-VI ₂	sN-VI ₄	sN-VI ₁₀
$\log q(\theta^*)$	$-\infty$	$-\infty$	15.5161	14.9543	14.6339	13.8562	15.1211
$\text{KL}[p^* q]$	$+\infty$	$+\infty$	3.1853	1.6967	3.8009	4.2452	0.8389

Table 2. Quality of fit of variational approximations on an RBF regression task.

References

1. Bishop, C.M.: Pattern recognition and machine learning. springer (2006)
2. Blundell, C., Cornebise, J., Kavukcuoglu, K., Wierstra, D.: Weight uncertainty in neural networks. arXiv preprint arXiv:1505.05424 (2015)
3. Chen, C., Carlson, D., Gan, Z., Li, C., Carin, L.: Bridging the gap between stochastic gradient mcmc and stochastic optimization. In: Artificial Intelligence and Statistics, pp. 1051–1060 (2016)
4. Chen, C., Zhang, R., Wang, W., Li, B., Chen, L.: A unified particle-optimization framework for scalable bayesian sampling. arXiv preprint arXiv:1805.11659 (2018)
5. Dhamala, J., Arevalo, H.J., Sapp, J., Horáček, B.M., Wu, K.C., Trayanova, N.A., Wang, L.: Quantifying the uncertainty in model parameters using gaussian process-based markov chain monte carlo in cardiac electrophysiology. Medical image analysis **48**, 43–57 (2018)
6. Gal, Y., Ghahramani, Z.: Dropout as a bayesian approximation: Representing model uncertainty in deep learning. In: international conference on machine learning, pp. 1050–1059 (2016)
7. Gong, W., Li, Y., Hernández-Lobato, J.M.: Meta-learning for stochastic gradient mcmc. arXiv preprint arXiv:1806.04522 (2018)
8. Heinrich, M.P., Simpson, I.J., Papież, B.W., Brady, M., Schnabel, J.A.: Deformable image registration by combining uncertainty estimates from supervoxel belief propagation. Medical image analysis **27**, 57–71 (2016)
9. Huszár, F.: Variational inference using implicit distributions. arXiv preprint arXiv:1702.08235 (2017)

10. Iglesias, J.E., Sabuncu, M.R., Van Leemput, K., Initiative, A.D.N., et al.: Improved inference in bayesian segmentation using monte carlo sampling: Application to hippocampal subfield volumetry. *Medical image analysis* **17**(7), 766–778 (2013)
11. Kennedy, M.C., O’Hagan, A.: Bayesian calibration of computer models. *Journal of the Royal Statistical Society: Series B (Statistical Methodology)* **63**(3), 425–464 (2001)
12. Konukoglu, E., Relan, J., Cilingir, U., Menze, B.H., Chinchapatnam, P., Jadidi, A., Cochet, H., Hocini, M., Delingette, H., Jaïs, P., et al.: Efficient probabilistic model personalization integrating uncertainty on data and parameters: Application to eikonal-diffusion models in cardiac electrophysiology. *Progress in biophysics and molecular biology* **107**(1), 134–146 (2011)
13. Le Folgoc, L., Delingette, H., Criminisi, A., Ayache, N.: Quantifying registration uncertainty with sparse bayesian modelling. *IEEE Transactions on Medical Imaging* **36**(2), 607–617 (2017)
14. Louizos, C., Welling, M.: Multiplicative normalizing flows for variational bayesian neural networks. In: *Proceedings of the 34th International Conference on Machine Learning-Volume 70*, pp. 2218–2227. JMLR. org (2017)
15. Miller, A.C., Foti, N.J., Adams, R.P.: Variational boosting: Iteratively refining posterior approximations. In: *Proceedings of the 34th International Conference on Machine Learning-Volume 70*, pp. 2420–2429. JMLR. org (2017)
16. Minka, T.P.: Expectation propagation for approximate bayesian inference. arXiv preprint arXiv:1301.2294 (2013)
17. Mirams, G.R., Pathmanathan, P., Gray, R.A., Challenor, P., Clayton, R.H.: Uncertainty and variability in computational and mathematical models of cardiac physiology. *The Journal of physiology* **594**(23), 6833–6847 (2016)
18. Patenaude, B., Smith, S.M., Kennedy, D.N., Jenkinson, M.: A bayesian model of shape and appearance for subcortical brain segmentation. *Neuroimage* **56**(3), 907–922 (2011)
19. Risholm, P., Janoos, F., Norton, I., Golby, A.J., Wells III, W.M.: Bayesian characterization of uncertainty in intra-subject non-rigid registration. *Medical image analysis* **17**(5), 538–555 (2013)
20. Schultz, S., Handels, H., Ehrhardt, J.: A multilevel Markov Chain Monte Carlo approach for uncertainty quantification in deformable registration. In: E.D. Angelini, B.A. Landman (eds.) *Medical Imaging 2018: Image Processing*, vol. 10574, pp. 162 – 169. International Society for Optics and Photonics, SPIE (2018). DOI 10.1117/12.2293588. URL <https://doi.org/10.1117/12.2293588>
21. Shi, J., Sun, S., Zhu, J.: Kernel implicit variational inference. arXiv preprint arXiv:1705.10119 (2017)
22. Srivastava, N., Hinton, G., Krizhevsky, A., Sutskever, I., Salakhutdinov, R.: Dropout: a simple way to prevent neural networks from overfitting. *The journal of machine learning research* **15**(1), 1929–1958 (2014)
23. Sun, S., Chen, C., Carin, L.: Learning structured weight uncertainty in bayesian neural networks. In: *Artificial Intelligence and Statistics*, pp. 1283–1292 (2017)
24. Tallec, C., Blier, L.: PyVarInf (2018). URL <https://github.com/ctallec/pyvarinf>
25. Tran, D., Ranganath, R., Blei, D.M.: Deep and hierarchical implicit models. arXiv preprint arXiv:1702.08896 **7**, 3 (2017)
26. Zhang, C., Bütepage, J., Kjellström, H., Mandt, S.: Advances in variational inference. *IEEE transactions on pattern analysis and machine intelligence* **41**(8), 2008–2026 (2018)